

Biomechanical role of peri-implant trabecular structures during vertical loading

Takashi Ohashi · Satoru Matsunaga · Ken Nakahara ·
Shinichi Abe · Yoshinobu Ide · Yuichi Tamatsu ·
Naoki Takano

Received: 14 May 2009 / Accepted: 30 July 2009 / Published online: 18 August 2009
© Springer-Verlag 2009

Abstract The aim of this study was to identify the load transfer paths in cortical bone and trabecular structure of cancellous bone in the jawbones for loads from endosseous implants. Maxillae were resected from beagle dogs 6 months after implant surgery and imaged using micro-computed tomography (micro-CT). A three-dimensional structure was produced based on the CT data and peri-implant trabecular structure was observed. Load transfer paths were analyzed from the results of three-dimensional finite element analysis. Furthermore, buffer actions in bone trabeculae when strain increased during stress analysis and when loads were applied were observed. Peri-implant bone trabeculae were seen extending into the upper and lower cortical bone from the fixture. The direction of bone trabecular alignment corresponded with the load transfer paths. In addition, analysis with increased strain confirmed that trabecular structures could serve as load buffers. These results suggest that bone trabeculae supporting load transfer from implants undergo remodeling.

Keywords Dental implant · Dog · Finite element method · Load transfer paths · Micro-CT · Trabecular structure

Introduction

Various biomechanical studies have determined the load applied to the surrounding bone by implants and the resulting stress occurring in peri-implant bone [1]. Duyck et al. reported crater-shaped defects in peri-implant bone when a transverse force was applied to the implants in a study using rabbits [2]. Kitamura et al. performed a biomechanical study on jawbones and implants using a simulation model and found that application of lateral load may result in implant failure [3]. However, in the simulation models used in these studies, cancellous bone structure was simplified as a block, and relationships between load arising from the implant and actual structure of the surrounding cancellous bone were not examined [4, 5]. With the development of micro-computed tomography (CT) and improved performance of analytical systems, it is now possible to conduct biomechanical analysis taking into consideration the actual morphology and structure of cancellous bone [6, 7]. Takano et al. reported differences in strength based on cancellous bone alignment in vertebral bone using this method [8]. To analyze the strength of peri-implant jawbone, biomechanical investigations based on the trabecular structure of cancellous bone are also necessary. Stegaroiu et al. compared the effect of loads from implants on the mandible when the trabecular structure of cancellous bone was simplified as a block and when the actual structure was analyzed. They reported that, in the actual trabecular structure, stress was dispersed over a wide area [9]. Matsunaga et al. reported a large concentration of stress in surrounding cancellous bone

T. Ohashi · S. Matsunaga (✉) · K. Nakahara · S. Abe · Y. Ide
Department of Anatomy, Tokyo Dental College,
Chiba, Japan
e-mail: matsuna@tdc.ac.jp

S. Matsunaga · S. Abe
Oral Health Science Center hrc7, Tokyo Dental College,
Chiba, Japan

Y. Tamatsu
Department of Neurology Gross Anatomy, Kagoshima University
Graduate School of Medical and Dental Sciences,
Kagoshima, Japan

N. Takano
Department of Mechanical Engineering, Keio University,
Yokohama, Japan

trabeculae due to load transfer from the implant to the mandible using a micro-CT image model that considered the actual cancellous bone structure of the mandible with a long-term embedded implant [10]. In the abovementioned studies, however, tensile stress and compressive stress were indicated in different colors, and sizes were given only in numerical values. Load transfer paths from the implant into cancellous bone remained unclear. Yamada et al. reported new bone formation in areas where loads were applied in peri-implant bone trabeculae [11]. It is thus important to know the direction of load dispersion in cancellous bone for determining the realignment of cancellous bone. The aim of the present study was to identify the load transfer paths in jawbone for loads arising from endosseous implants using a system that displays load direction.

Materials and methods

Animals

Two 12-month-old male beagle dogs (body weight, 10–15 kg) with no physical abnormalities were used 1 week after introduction into the experiment. The animal study was conducted based on the ethical regulations for animal studies at Tokyo Dental College.

Surgical procedure

Before starting the experiment, 5% ketamine hydrochloride (Ketalar 50 Intramuscular for veterinary use; Sankyo, Tokyo, Japan) was administered intramuscularly at 0.2 mg/kg as premedication. General anesthesia was then induced by intravenous administration of 5% pentobarbital sodium (Nembutal injection solution; Dainippon Pharmaceutical, Osaka, Japan) at 0.5 ml/kg. Infiltration anesthesia using 2% xylocaine (Dental Xylocaine; Fujisawa Pharmaceutical, Osaka, Japan) was also applied to the operation site. After disinfection around the mouth and oral cavity with 0.5% benzalkonium chloride (Benzalkonium chloride solution; Kozakai Pharmaceutical, Tokyo, Japan), the operation was performed. Gingival crevicular incisions were made and mucoperiosteal flaps were raised. The tooth roots were then divided by a diamond disk and diamond bur under irrigation with sterile physiological saline solution. Finally, bilateral maxillary fourth premolars, first molars, and second molars were extracted using tooth extraction forceps. After a 3-month recovery period, three implants in total were surgically placed in the left maxillary molar region. Regular neck-type SLA implants (Straumann, Basel, Swiss) with a diameter of 4.1 mm and height of 6 mm were placed. An incision into the periosteum was made on the alveolar crest, and mucoperiosteal flaps were

raised. The implant sites were prepared using pilot drills of diameters 2.2 mm, 2.8 mm, and 3.5 mm, in that order, under irrigation with sterile physiological saline solution. Adapter taps were then formed under irrigation with sterile physiological saline solution, and the implant (fixture) was inserted. Healing caps were placed on the endosseous implants, and the operating field was washed with sterile physiological saline solution. Mucoperiosteal flaps were sutured so that only the healing caps were exposed. Implants were placed at equal distances in the mesiodistal direction. After 3 months, a crown connecting the three implants was attached. The superstructure of the implant was prepared using a 12% gold–silver–palladium alloy (Kinpara S12; Ishifuku, Tokyo, Japan). These implants were not shaped like the natural teeth of the dogs, but, instead, were simple cylindrical structures that could be maintained in a hygienic condition. It was ensured that the right molar region was not used for tearing. The occlusal surface of the superstructure was prepared to occlude with the antagonist teeth at 2–3 points (Fig. 1). After attachment, the dogs were given solid dog food, and plaque control was not performed during the experimental period. All dogs were sacrificed 3 months later, and the maxillae were resected (Fig. 2).

Micro-CT imaging

Images of samples were taken using a micro-CT system (HMX-225-Actis4; Tesco, Tokyo, Japan). The imaging intensifier (II) of the micro-CT was 4 in. in size and had a 1-in. 16-bit CCD camera with 1,024×1,024 scanning lines. Using this camera, 1,200 images were obtained as raw data. Based on these data, two-dimensional slice data were

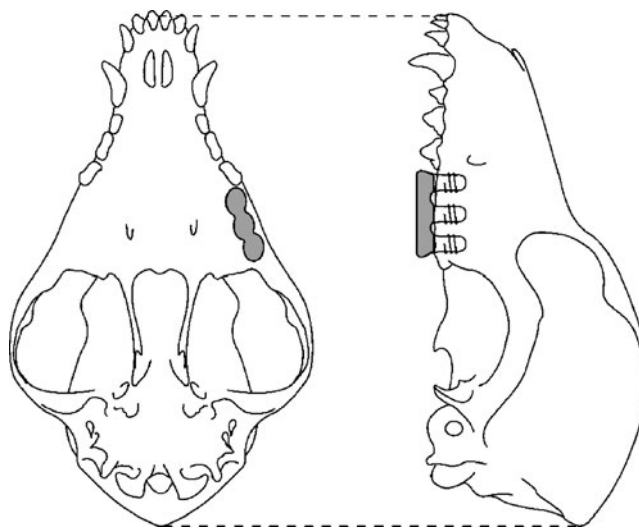


Fig. 1 Schematic drawing of the implant superstructure

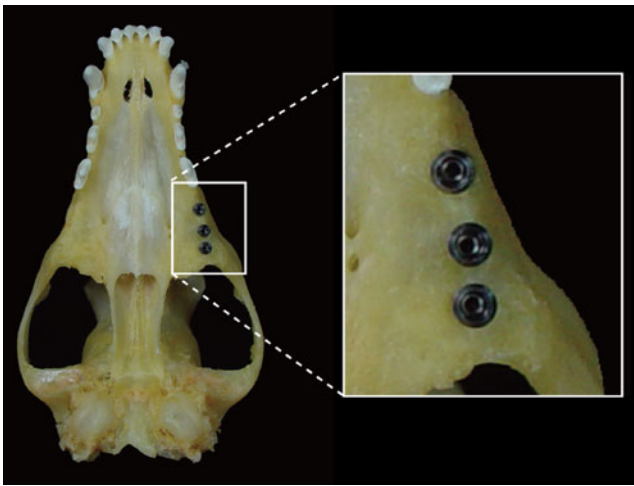


Fig. 2 Samples including the implants at left molar regions

prepared using the back-projection method. The standard horizontal plane was the plane passing through three points: the contact point between the left and right maxillary central incisors and the centers of the left and right external auditory foramens. The standard vertical plane was the plane orthogonal to the standard horizontal plane and passing through the posterior-most points of the left and right third premolars. Based on these standard planes, micro-CT imaging was performed from the posterior-most point of the third premolar to the posterior-most point of the maxillary alveolar process (Fig. 3). Imaging conditions were: matrix size, 512×512; tube voltage, 100 kV; tube current, 70 μA; magnification, ×6.7; slice width, 20 μm; slice pitch, 20 μm; field of reconstruction, 26 mm; and voxel size, 52×52×20 μm.

Fig. 3 Standard planes: **a** the horizontal plane (occlusal plane); **b** the plane parallel to the occlusal plane passing through the inferior-most point of the infraorbital foramen; **c** the vertical plane against the occlusal plane passing through the posterior-most points of the left and right third premolars; **d** the vertical plane passing through the maxillary alveolar process

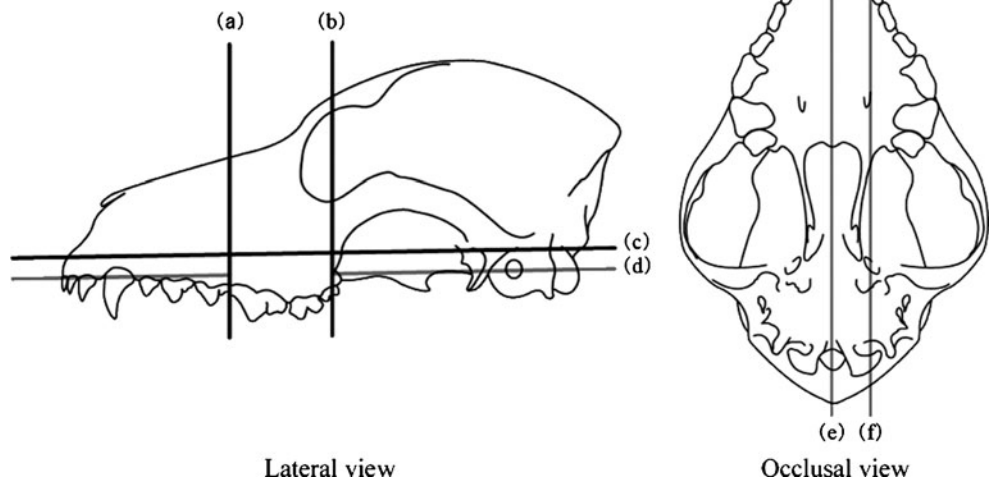


Image processing for structural observations

Bone structure was observed using the slice data obtained. Images were constructed by the volume-rendering method from slice data using three-dimensional (3D) construction software (VG Studio; Volume Graphics, Heidelberg, Germany).

Image processing for stress analysis and analysis during vertical loading

Micro-CT images were first subjected to noise elimination. Binarization was then performed using thresholds obtained by discrimination analysis. After labeling, images were automatically converted to 8-node hexahedrons. In the boundaries between implants and bone, areas of contact were considered connected. The number of voxel elements in the region connecting the implant and bone was about 4 million.

Model components were bone and implants, both considered as linear isotropic materials. Using previously reported values of mechanical properties as reference, the Young’s modulus and the Poisson ratio for bone were set at 15 GPa and 0.30, respectively, and those for implants at 115 GPa and 0.35, respectively.

The plane parallel to the occlusal plane passing through the inferior-most point of the infraorbital foramen (standard horizontal plane in micro-CT analysis) was set as the boundary condition at the restrained area. The element on this surface was restrained by 1 voxel.

Load conditions included a 1-voxel surface load region with three implant superstructures as one surface, and a 10-N vertical load in total was applied (Fig. 4).

Areas for analysis were within the CT imaging range.

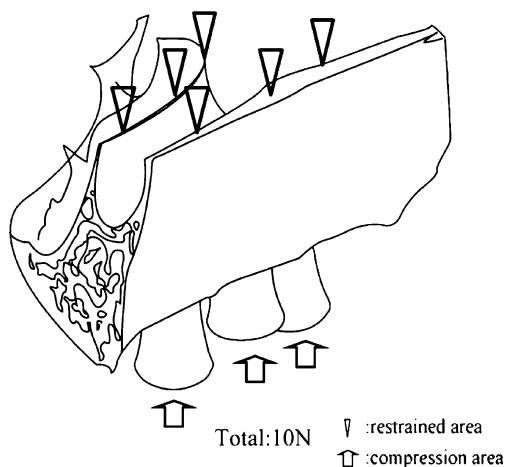


Fig. 4 Load condition and restrained surface

Stress analysis during vertical loading was performed using three-dimensional finite element software (Voxelcon; Quint, Tokyo, Japan). Load transfer paths in trabeculae were observed using DoctorBQ (KGT, Tokyo, Japan, and Quint, Tokyo, Japan) as output.

The deformation mode with strain increased by 5,000-fold was observed dynamically to examine the mechanical role of cancellous bone.

Results

Bone morphological observations and analysis of trabecular structure

1. Observation of trabecular structure

Figure 5 shows trabecular structures diffusing radially from around the fixture and extending to the surrounding cortical bone and adjacent fixtures.

Trabecular structures connecting the fixtures were obvious in Figs. 5 and 6.

Bone trabeculae at the upper region of the fixture root appeared to connect the fixture and upper cortical bone in a truncated cone manner. Trabeculae extending into the upper cortical bone and lower cortical bone were observed around fixtures. Trabeculae extending into the upper cortical bone were cross-linked and connected with trabeculae extending into lower cortical bone.

Stress analysis during vertical loading

1. Load transfer paths

Stress was assessed with emphasis on the distribution of maximum principal stress. The principal stress vector for all elements was expressed stereoscopically to confirm load transfer paths from implants.

Compression stress was transferred into the fixture reaching the trabecular structures at the upper region of the fixture root and around the fixture, then diffusing into the upper cortical bone (Fig. 7). The direction of transfer basically corresponded with the direction of trabecular alignment.

Tensile stress was generated between fixtures and transferred to the lower cortical bone from fixtures. The direction of transfer between fixtures was mainly mesio-distal (Fig. 8).

2. Deformation mode

Deformation mode with strain increased by 5,000-fold was derived from the results of finite element analysis, and the type of deformation occurring in the trabecular structure due to the applied load was investigated.

Bone trabeculae extending to the upper cortical bone were compressed, but trabeculae extending to the lower cortical bone were stretched (Fig. 9).

Discussion

In the Consensus Development Conference Statement published by the National Institutes of Health in 2000,

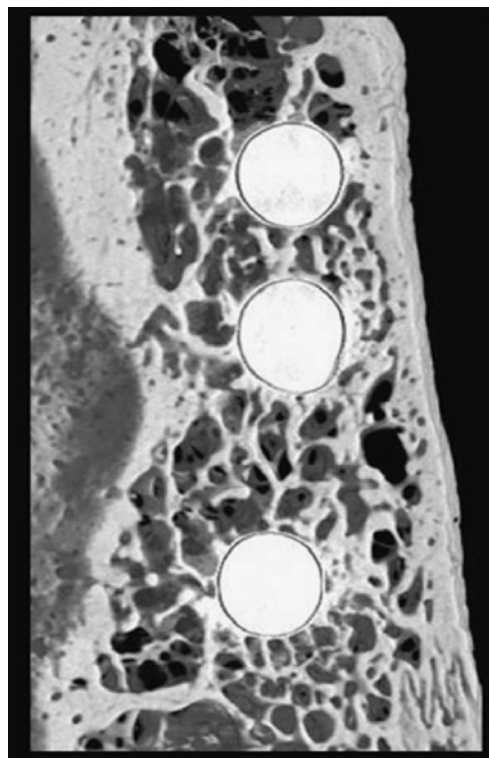
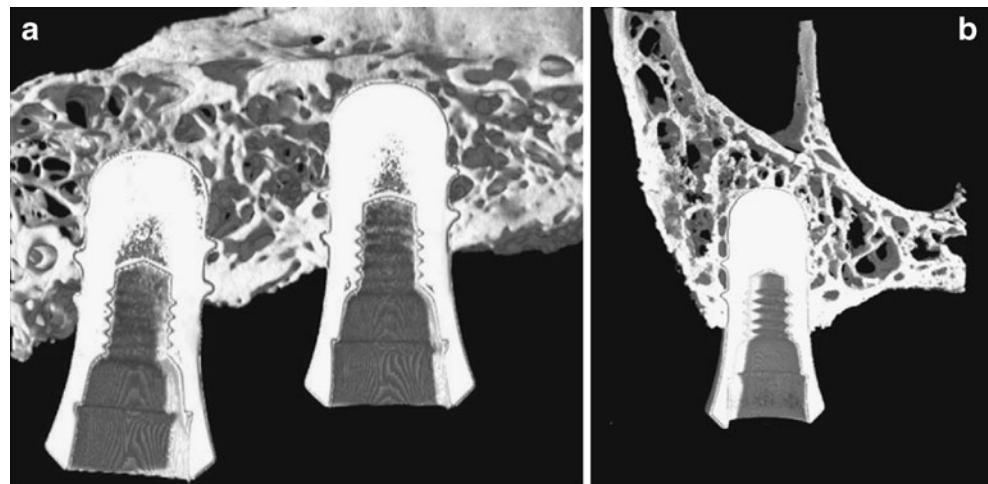


Fig. 5 Reconstructed 3D image: the occlusal section cut at the middle of center fixture. Trabeculae can be seen radially arranged around the implant. The adjacent implants are connected by thick trabecular structures

Fig. 6 Reconstructed 3D images: **a** mesiodistal section; **b** buccolingual section. **a** Shows the trabecular structures connecting the implant to the upper cortical bone (nasal side) as well as the trabeculae connecting the implant to the lower region (palatal and buccal regions). **b** Cancellous bone trabecular structures can be seen arranged around the implant



standards for bone quality were proposed in addition to the conventional evaluation of bone density as numerous factors including cancellous bone trabecular structure affect bone strength [12]. Performing analysis based on the actual cancellous bone morphology and structure is thus important to determine bone strength in detail. In the present study, the characteristics of trabecular structure were evaluated by reproducing the cancellous bone trabecular structure based on micro-CT data and determining load transfer paths.

Kong et al. reported that stress distribution generated in peri-implant bone differs with the direction and type of load applied to the implant, but stress is concentrated mainly in cortical bone around the neck part of the implant [13]. The present study showed that, in patients with thin cortical bone in areas such as the upper alveolar region, cancellous bone trabeculae between implants act as a bridge between cortical bones and disperse stress by forming load transfer paths. Cancellous bone around implants usually disperses stress to the cortical bone, but, when stress cannot be adequately dispersed, strength is assured by remodeling of the trabecular structure to match the load transfer direction.

Peri-implant bone trabeculae, as used in the present analysis, received mechanical stimulation from the mandible because the implant was in contact with the antagonist teeth. Parfitt et al. reported that cell activity called remodeling rotation (consisting of cessation, resorption, and formation) occurs on the surface of bone trabeculae under mechanical stimulation and that remodeling occurs in response to stimulation [14, 15]. Using a simulation model, Huiskes et al. suggested that the trabecular structure of cancellous bone is aligned in accordance with the load [16]. The trabecular structure observed in the present study showed a cross-linked structure consisting of bone trabeculae extending into the upper cortical bone and bone trabeculae extending into the implant as a result of mechanical stimulation (Figs. 5 and 6). The results of finite element analysis of load transfer paths occurring within bone revealed that the trabecular structures extending to the upper cortical bone generate compressive stress while the ones extending to the lower cortical bone generate tensile stress in response to loads. By specifying the directions of the load as vectors in this study, it became obvious that the

Fig. 7 Load transfer path at the mesiodistal section: **a** the image reconstructed by Doctor BQ; **b** the simplified image (blue arrow: compression stress, red arrow: tensile stress)

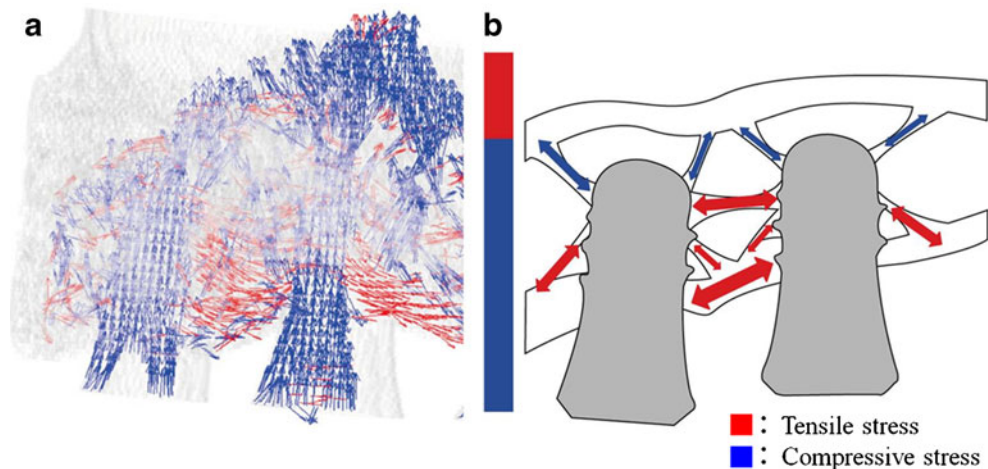
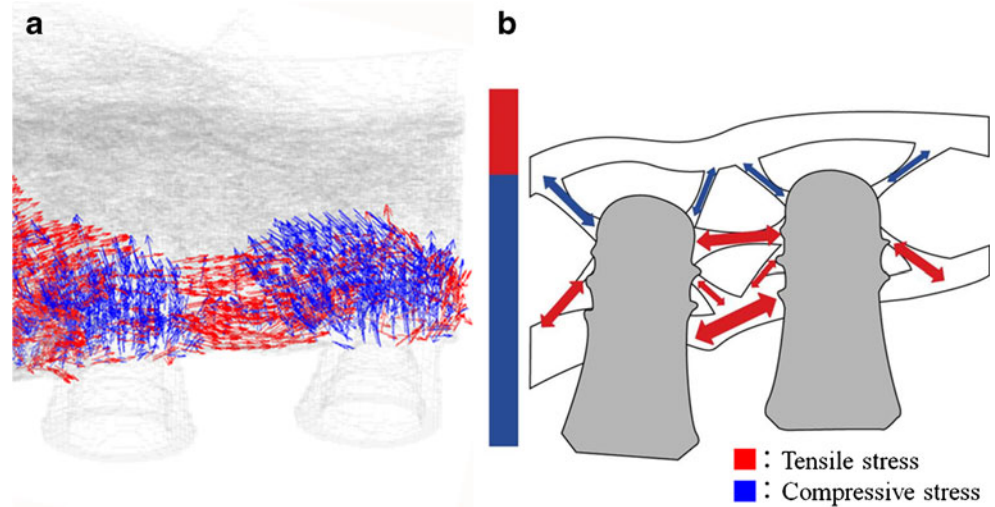


Fig. 8 Load transfer path at the occlusal section: **a** the image reconstructed by Doctor BQ; **b** the simplified image (*blue arrow: compression stress, red arrow: tensile stress*)

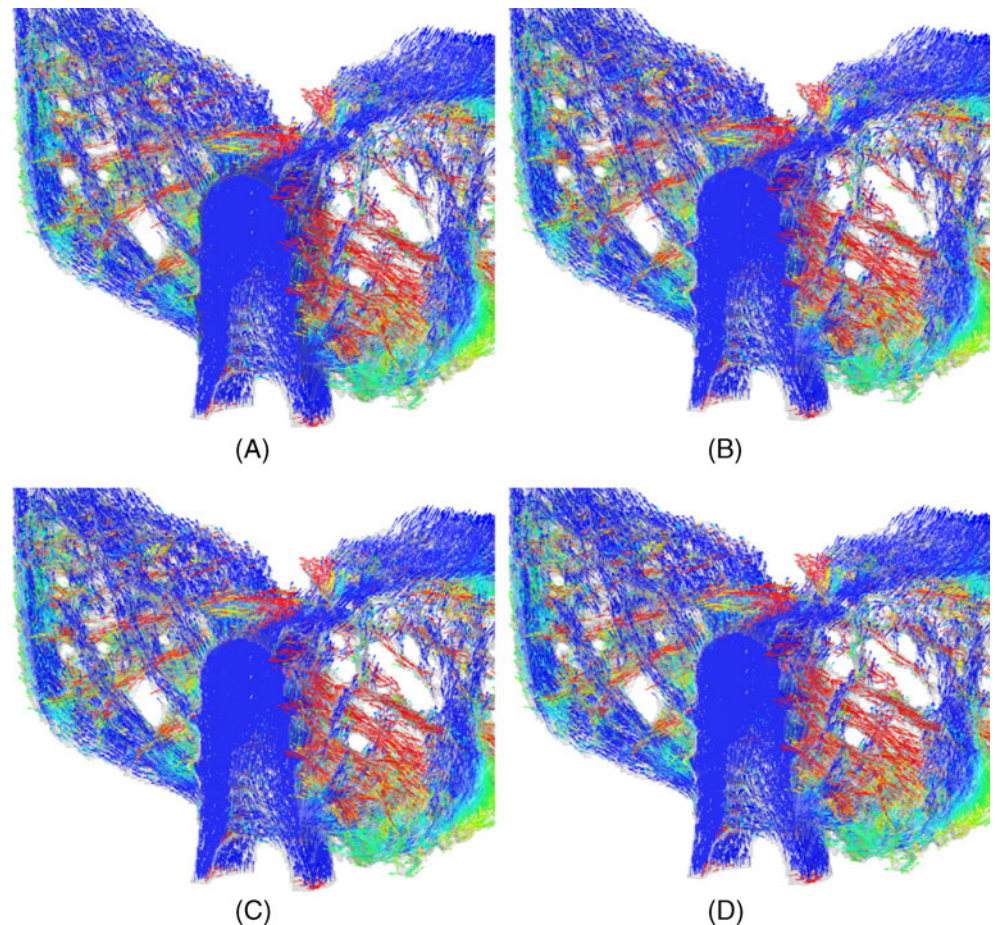


direction of transmission of the load and its distribution within the bone trabecular structure were homologous. This indicated that the bone trabecular structure which was realigned by mechanical stimulus had a morphology that dispersed the load from implants to cortical bone. Furthermore, the results of the analysis in deformation mode showed that cross-linked trabecular structures buffer the

load from implants. These results implied that trabeculae not only remodel and disperse the load from the implant to the cortical bone but also transform themselves into a shock-absorbing structure.

At present, examination of trabecular structure of cancellous bone is rarely performed prior to implant surgery. Surgeons make decisions based on their own discretion and choose the

Fig. 9 Each stage of deformation occurring in the trabecular structure due to the applied load in order from **a** to **d**



surgical method best suited to each patient's bone hardness [17, 18]. Recently, bone density and bone mineral content have been evaluated preoperatively in some cases in consideration of the risk of stress concentration around fixtures after implant operations. In addition to these analyses, examination of the structural properties of cancellous bone including stress analysis would be useful in predicting acceptable loads of endosseous implants. Furthermore, since newly realigned bone trabeculae around implants have been suggested to be involved in the support of functional pressure, long-term follow-up is warranted after implant surgery.

Acknowledgments The authors would like to thank Dr. Mitsuteru Asai and Mr. Kunihiko Taki of the Department of Micro System Technology, Faculty of Science and Engineering, Ritsumeikan University, for providing valuable technical information. We also thank Professor Masatsugu Hashimoto of the Department of Forensic Anthropology, Tokyo Dental College, for his thoughtful review of the manuscript. The authors also appreciate the enthusiastic cooperation of the staff of the Department of Anatomy, Tokyo Dental College. This study was supported by grants to Satoru Matsunaga (19890223, 20791441) from the Ministry of Education, Science, Sport, Culture and Technology of Japan.

Conflict of interests The authors have no financial relationship with the organization that sponsored the research.

References

- Eraslan O, Inan O (2009) The effect of thread design on stress distribution in a solid screw implant: a 3D finite element analysis. *Clin Oral Investig*, June 20 [Epub ahead of print] doi:10.1007/s00784-009-0305-1
- Duyck J, Rønold HJ, Van Oosterwyck H et al (2001) The influence of static and dynamic loading on marginal bone reactions around osseointegrated implants: an animal experimental study. *Clin Oral Implants Res* 12:207–218
- Kitamura E, Stegaroiu R, Nomura S et al (2004) Biomechanical aspects of marginal bone resorption around osseointegrated implants. Considerations based on a three-dimensional finite element analysis. *Clin Oral Implants Res* 15:401–412
- Liang K, Yingying S, Kaijin H et al (2008) Selections of the cylinder implant neck taper and implant end fillet for optimal biomechanical properties. A three-dimensional finite element analysis. *J Biomech* 41:1124–1130
- Ming LH, Fang CC, Hung CK et al (2007) Influence of off-axis loading of an anterior maxillary implant. A 3-dimensional finite element analysis. *Int J Oral Maxillofac Implants* 22:301–309
- Müller R, Rügsegger P (1997) Micro-tomographic imaging for the nondestructive evaluation of trabecular bone architecture. *Stud Health Technol Inform* 40:61–79
- Ulrich D, Hildebrand T, Van RB et al (1997) The quality of trabecular bone evaluated with micro-computed tomography, FEA and mechanical testing. *Stud Health Technol Inform* 40:97–112
- Takano N, Nakano T, Umakoshi Y et al (2007) High-resolution image-based simulation of biological hard tissues. *Materia Japan* 7:456–459
- Stegaroiu R, Watanabe N, Tanaka M et al (2006) Peri-implant stress analysis in simulation models with or without trabecular bone structure. *Int J Prosthodont* 19:40–42
- Matsunaga S, Okudera H, Abe S et al (2008) The influence of bite force on the internal structure of the mandible through implant. *J Oral Biosci* 50:194–199
- Yamada A, Yamakura D, Kishi M (2005) Three-dimensional observation of internal structure of canine mandible by microcomputed tomography. Morphometric differences between loaded and unloaded cancellous bone around implants. *Shikwa Gak* 105:577–587
- NIH Consensus Development Panel on Osteoporosis Prevention, Diagnosis, and Therapy. March 7-29, 2000: highlights of the conference. *South Med J* 2001;94:569–573
- Kong L, Sun Y, Hu K et al (2008) Selections of the cylinder implant neck taper and implant end fillet for optimal biomechanical properties. A three-dimensional finite element analysis. *J Biomech* 41:1124–1130
- Lee KI, Roh HS, Yoon SW (2003) Acoustic wave propagation in bovine cancellous bone: application of the modified Biot-Attenborough model. *J Acoust Soc Am* 114:2284–2293
- Parfitt AM (1994) Osteonal and hemi-osteonal remodeling: the spatial and temporal framework for signal traffic in adult human bone. *J Cell Biochem* 55:273–286
- Huiskes R, Weinans H, Grootenboer HJ et al (1987) Adaptive bone-remodeling theory applied to prosthetic-design analysis. *J Biomech* 20:1135–1150
- Lekholm U, Zarb GA (1985) Patient selection and preparation. In: Branemark P-I, Zarb GA, Albrektsson T (eds) *Tissue-integrated prostheses. Osseointegration in clinical dentistry*. Quintessence, Chicago, pp 199–209
- Misch CE (1990) Density of bone: effect on treatment plans, surgical approach, healing, and progressive bone loading. *Int J Oral Implantol* 6:23–31